A Numerical Model with Finite Difference Schemes for Multi-Species Solute Transport in Porous Media

Amin GHAREHBAGHI

Hasan Kalyoncu University, Faculty of engineering, Civil Engineering Department, Şahinbey, Gaziantep, Turkey

Email: amin.gharehbaghi@hku.edu.tr,

*Corresponding Auth*or: gharehbaghi.amin@gmail.com

ABSRACT

A precise forecast of contaminant and solute transport has an inevitable role in water resources management. In line with this purpose, in this paper, a novel one-dimensional numerical model is proposed for the transmission of a decay chain through homogeneous porous media. To develop the suggested model, two different schemes of the finite difference method, namely the Lax-Wendroff scheme and the Fourth-Order scheme, are used. The verification and validation of the established model are examined by the analytical results of three multi-species solute dispersion problems with three- and four-chain members. The total mean square error, L2- and L∞-norms are applied to assess the results. Although analyses show that both schemes provided reliable results, the numerical results of the Lax-Wendroff scheme are more accurate.

INTRODUCTION

To manage surface- and groundwater resources, estimating the contaminant and solute transport phenomenon is significant. Some researchers have conducted experimental studies or developed numerical methods for groundwater problems (Kaya and Arisoy 2011; Celiker 2016; Dalkiliç and Gharehbaghi 2021). There are benefits in considering the phenomenon of pollutant and solute transport when examining groundwater problems. Each year by increasing the contamination of aquifers with substances such as pesticides, chlorinated solvents, and petroleum hydrocarbons the investigation of the safety of water resources becomes more significant. The transport processes of some solutes and contaminants are usually more complicated than a first-order or pseudo-first-order decay. Thus, a single-member transport model cannot predict the transformation process from the parent species to the daughter species. So far, most researchers have focused on the analytical and numerical models that could describe the phenomenon of single-member transport of various contaminants. (Kumar et al., 2010; Savovic et al., 2011; Savovic and Djordjevich 2012 & 2013; Singh et al., 2012; Gharehbaghi 2016 & 2017; Das et al., 2018; among many). On the other hand, most analytical solutions have limited applications. "One of the points of emphasis for analytical expressions is that application of an analytical solution is strongly affected by initial and boundary conditions. Therefore, many difficulties can encounter when dealing with complex geometries" (Gharehbaghi 2017). Three classical methods, including finite difference method (FDM), finite element method (FEM), and finite volume method (FVM), are among the most favorite numerical methods. To the best of our knowledge, FDM is the most applied numerical technique in engineering. Therefore, this method is employed to develop a new numerical model. Reviews of several studies in one-dimensional (1D) form regarding this paper are yielded here.

Chen-Charpentier et al., (2009) suggested a numerical model for simulating the water flow, the transport of a contaminant and nutrients, plus the progress of biofilm-forming microbes and biodegradation microbes in porous media for different kinetics. They announced that the governing equation was solved using mixed-finite elements and a non-standard method. Natarajan and Kumar (2010) developed an alternative approach to the decomposition method with implicit FDM for solving multispecies transport in porous media coupled with first-order reactions. Ramos et al., (2011) used HYDRUS-1D software and exerted various experimental studies to predict soil sodification and salinization possibilities. They solved the equations with Galerkin-type linear FEM. Torlapati (2013) proposed a multi-component reactive transport model by using explicit forms of backward difference FDM, total variation diminishing schemes, and fully implicit approaches to predict the fate and transport of biochemical and geochemical reactive transport problems in a 1D condition. Bagalkot and Kumar (2015) introduced a 1D numerical assessment with FDM for multispecies radionuclide transport in a single-horizontal coupled fracture-matrix system. Sharma et al. (2016) investigated the impact of distance-dependent dispersion on multispecies solute transport process with upwind- and central-difference approaches of implicit FDM and with constant, linear, and exponential dispersivity functions. Zhang et al., (2018) proposed a 1D model for multi-component solute transport in saturated soil based on the modified diffusion and the modified competitive Langmuir adsorption equations. They used the FEM-based software COMSOL Multiphysics to assess the outcomes. Pathania et al., (2020) recommended a numerical model based on the meshless element-free Galerkin method to calculate groundwater flow and multispecies reactive transport coupled with sequential decay reactions in unconfined aquifers. They analyzed the outcomes of the recommended model using FDM, FEM, and MODFLOW-RT3D.

This paper presents the implementation and results of a novel numerical model to predict the multi-species solute transport phenomenon in 1D form with the Advection-Dispersion Equation (ADE). The proposed model used two robust FDM schemes, including Lax Wendroff Finite Difference Method (LWFDM) and Fourth Order Finite Difference Method (FOFDM). Finally, three analytical solutions from two separate studies of Bauer et al., (2001) and Pérez Guerrero et al., (2009) are applied to evaluate the performance of the proposed model.

Transport model

Sequential chemical intermediates or radionuclides, coupled with first-order decay processes, form a decay chain. The general pattern of sequential multi-species solute transport in porous media can be described using the following equation. (Bauer et al. 2001; Pérez Guerrero et al. 2009).

$$R_m \frac{\partial c_m}{\partial t} = D \frac{\partial^2 c_m}{\partial x^2} - v \frac{\partial c_m}{\partial x} - R_m \lambda_m c_m + R_{m-1} \lambda_{m-1} c_{m-1}; \quad m = 1, \dots., M; \quad \lambda_0 = 0; \quad 0 <$$

$$x < \infty; \quad t > 0; \tag{1}$$

where c_m, R_m, D, v, λ_m, x, and t are the concentration of the mth member of the decay chain formed by M species, the retardation coefficient for the mth species, the dispersion coefficient, the constant pore water velocity, the first-order decay constant for the mth species, the longitudinal axis, and time, respectively. The phrase '$R_m \lambda_m$' is replaced by the indication of k_m for simplification.

Numerical solution

As noted previously, two schemes of FDM (i.e., LWFDM and FOFDM) are employed to solve the multi-species solute transport in porous media. For a start, by replacing the value of m as one in Eq. (1) (i.e., $m=1$), the required equation for the first member is given as follows:

$$R_1 \frac{\partial c_1}{\partial t} = D \frac{\partial^2 c_1}{\partial x^2} - v \frac{\partial c_1}{\partial x} - k_1 C_1 \quad 0 < x < \infty, \quad t > 0 \tag{2}$$

In this step, the numerical solution of LWFDM is provided for the first-member. Consider the following approximations of the derivatives for the first- and second-order.

$$\frac{\partial C_1}{\partial x} = (1 - \emptyset)\frac{C_{1_i}^t - C_{1_{i-1}}^t}{\Delta x} + \emptyset\frac{C_{1_{i+1}}^t - C_{1_i}^t}{\Delta x} \tag{3}$$

$$\frac{\partial^2 C_1}{\partial x^2} = \frac{C_{1_{i+1}}^t - 2C_{1_i}^t + C_{1_{i-1}}^t}{\Delta x^2} \tag{4}$$

$$\frac{\partial C_1}{\partial t} = \frac{C_{1_i}^{t+1} - C_{1_i}^t}{\Delta t} \tag{5}$$

And the solution domain of the problem is divided by a mesh of grid lines as follows:

$$x_i = i\Delta x \qquad i = 0,1,2,\dots,N_x \tag{6}$$

$$t_s = s\Delta t \qquad s = 0,1,2,\dots,N_t \tag{7}$$

By employing Eqs. (3–5), the solution of the first-member (i.e., Eq. (2)) for LWFDM is written as follows:

$$R_1\frac{C_{1_i}^{t+1} - C_{1_i}^t}{\Delta t} = D\frac{C_{1_{i+1}}^t - 2C_{1_i}^t + C_{1_{i-1}}^t}{\Delta x^2} - v\left((1-\emptyset)\frac{C_{1_i}^t - C_{1_{i-1}}^t}{\Delta x} + \emptyset\frac{C_{1_{i+1}}^t - C_{1_i}^t}{\Delta x}\right) - k_1 C_{1_i}^t \tag{8}$$

where the value of $\emptyset$ is equal to $\emptyset = \left.\left(1 - v\frac{\Delta t}{\Delta x}\right)\right/2 = \frac{1}{2} - v\frac{\Delta t}{2\Delta x}$ (Appadu, 2013). By some manipulation, Eq. (8) can rearrange as follows:

$$C_{1_i}^{t+1} = C_{1_{i-1}}^t\left(\frac{\Delta tD}{R_1\Delta x^2} + \frac{v\Delta t(1-\emptyset)}{R_1\Delta x}\right) + C_{1_i}^t\left(\frac{-2\Delta tD}{R_1\Delta x^2} - \frac{v\Delta t(1-\emptyset)}{R_1\Delta x} + \frac{v\Delta t\emptyset}{R_1\Delta x} - k_1\frac{\Delta t}{R_1} + 1\right) + C_{1_{i+1}}^t\left(\frac{\Delta tD}{R_1\Delta x^2} - \frac{v\Delta t\emptyset}{R_1\Delta x}\right)$$

$$\tag{9}$$

To calculate the LWFDM more easily, two coefficients, which we call m_m and n_m coefficients, are presented in total.

$$m_m = \frac{\Delta tD}{R_m.\Delta x^2} \tag{10}$$

$$n_m = \frac{\Delta tv}{R_m.\Delta x} \tag{11}$$

By replacing the m_1 and n_1 coefficients in Eq. (9), the final form of solution for the first-member for LWFDM is given as follows:

$$C_{1_i}^{t+1} = C_{1_{i-1}}^t\left(m_1 + n_1(1-\emptyset)\right) + C_{1_i}^t\left(-2m_1 - n_1(1-\emptyset) + n_1\emptyset - k_1\frac{\Delta t}{R_1} + 1\right) + C_{1_{i+1}}^t(m_1 - n_1\emptyset)$$

$$\tag{12}$$

By applying the similar solution steps, the final form of the solution for the second-, third- and fourth-species for LWFDM are extracted as follows:

$$C_{2_i}^{t+1} = C_{2_{i-1}}^t\left(m_2 + n_2(1-\emptyset)\right) + C_{2_i}^t\left(-2m_2 - n_2(1-\emptyset) + n_2\emptyset - k_2\frac{\Delta t}{R_2} + 1\right) + C_{2_{i+1}}^t(m_2 - n_2\emptyset) +$$

$$k_1\frac{\Delta t}{R_2}C_{1_i}^t \tag{13}$$

$$C_{3_i}^{t+1} = C_{3_{i-1}}^{t}\left(m_3 + n_3(1 - \emptyset)\right) + C_{3_i}^{t}\left(-2m_3 - n_3(1 - \emptyset) + n_3\emptyset - k_3\frac{\Delta t}{R_3} + 1\right) + C_{3_{i+1}}^{t}(m_3 - n_3\emptyset) +$$

$$k_2\frac{\Delta t}{R_3}C_{2_i}^{t} \tag{14}$$

$$C_{4_i}^{t+1} = C_{4_{i-1}}^{t}\left(m_4 + n_4(1 - \emptyset)\right) + C_{4_i}^{t}\left(-2m_4 - n_4(1 - \emptyset) + n_4\emptyset - \frac{\Delta t}{R_4}k_4 + 1\right) + C_{4_{i+1}}^{t}(m_4 - n_4\emptyset) +$$

$$k_3\frac{\Delta t}{R_4}C_{3_i}^{t} \tag{15}$$

In this step to solve Eq. (2) in EFOFDM form, for each time and space step, the derivatives of the first- and second-order are expressed as follows (Kaya and Gharehbaghi, 2014, Gharehbaghi et al., 2017):

$$\frac{\partial c_1}{\partial t} = \frac{c_{i-2} - 8c_{i-1} + 8c_{i+1} - c_{i+2}}{12\Delta x} \tag{16}$$

$$\frac{\partial^2 c_1}{\partial x^2} = \frac{-c_{i-2} + 16c_{i-1} - 30c_i + 16c_{i+1} - c_{i+2}}{12\Delta x^2} \tag{17}$$

$$\frac{\partial c_1}{\partial x} = \frac{C_{1_i}^{t+1} - C_{1_i}^{t}}{\Delta t} \tag{18}$$

To initiate the discretization, Eqs. (16-18) are replaced in Eq. (2).

$$R_1\frac{C_{1_i}^{t+1} - C_{1_i}^{t}}{\Delta t} = D\frac{-C_{1_{i-2}}^{t} + 16C_{1_{i-1}}^{t} - 30C_{1_i}^{t} + 16C_{1_{i+1}}^{t} - C_{1_{i+2}}^{t}}{12\Delta x^2} - v\frac{C_{1_{i-2}}^{t} - 8C_{1_{i-1}}^{t} + 8C_{1_{i+1}}^{t} - C_{1_{i+2}}^{t}}{12\Delta x} - k_1 C_{1_i}^{t} \tag{19}$$

Eqs. (6-7) have been used to generate the grid line. With some manipulation, the final form of the solution for the first-member is acquired as follows:

$$C_{1_i}^{t+1} = C_{1_{i-2}}^{t}\left(-\frac{\Delta tD}{12\Delta x^2 R_1} - \frac{\Delta tv}{12\Delta x R_1}\right) + C_{1_{i-1}}^{t}\left(\frac{16\Delta tD}{12\Delta x^2 R_1} + \frac{8\Delta tv}{12\Delta x R_1}\right) + C_{1_i}^{t}\left(-\frac{30\Delta tD}{12\Delta x^2 R_1} - \frac{\Delta tk_1}{R_1} + 1\right) +$$

$$C_{1_{i+1}}^{t}\left(\frac{16\Delta tD}{12\Delta x^2 R_1} - \frac{8\Delta tv}{12\Delta x R_1}\right) + C_{1_{i+2}}^{t}\left(-\frac{\Delta tD}{12\Delta x^2 R_1} + \frac{\Delta tv}{12\Delta x R_1}\right) \tag{20}$$

Similar to the solution of LWFDM, two coefficients, which we call ka_m and kb_m coefficients, are introduced to solve FOFDM more easily.

$$ka_m = \frac{\Delta tD}{12\Delta x^2 R_m} \tag{21}$$ $$kb_m =$$

$$\frac{\Delta tv}{12\Delta x R_m} \tag{22}$$

And the final form of discretization with FOFDM is rearranged as follows:

$$C_{1_i}^{t+1} = C_{1_{i-2}}^{t}(-ka_1 - kb_1) + C_{1_{i-1}}^{t}(16ka_1 + 8kb_1) + C_{1_i}^{t}\left(-30ka_1 - \frac{\Delta tk_1}{R_1} + 1\right) + C_{1_{i+1}}^{t}(16ka_1 - 8kb_1) +$$

$$C_{1_{i+2}}^{t}(-ka_1 + kb_1) \tag{23}$$

By applying a similar solution process, the ultimate form of the solution for second-, third- and fourth-species for FOFDM are extracted as follows:

$$C_{2_i}^{t+1} = C_{2_{i-2}}^{t}(-ka_2 - kb_2) + C_{2_{i-1}}^{t}(16ka_2 + 8kb_2) + C_{2_i}^{t}\left(-30ka_2 - \frac{\Delta t k_2}{R_2} + 1\right) + C_{2_{i+1}}^{t}(16ka_2 - 8kb_2) +$$

$$C_{2_{i+2}}^{t}(-ka_2 + kb_2) + \frac{\Delta t k_1}{R_2} C_{1_i}^{t} \tag{24}$$

$$C_{3_i}^{t+1} = C_{3_{i-2}}^{t}(-ka_3 - kb_3) + C_{3_{i-1}}^{t}(16ka_3 + 8kb_3) + C_{3_i}^{t}\left(-30ka_3 - \frac{\Delta t k_3}{R_3} + 1\right) + C_{3_{i+1}}^{t}(16ka_3 - 8kb_3) +$$

$$C_{3_{i+2}}^{t}(-ka_3 + kb_3) + \frac{\Delta t k_2}{R_3} C_{2_i}^{t} \tag{25}$$

$$C_{4_i}^{t+1} = C_{4_{i-2}}^{t}(-ka_4 - kb_4) + C_{4_{i-1}}^{t}(16ka_4 + 8kb_4) + C_{4_i}^{t}\left(-30ka_4 - \frac{\Delta t k_4}{R_4} + 1\right) + C_{4_{i+1}}^{t}(16ka_4 - 8kb_4) +$$

$$C_{4_{i+2}}^{t}(-ka_4 + kb_4) + \frac{\Delta t k_3}{R_4} C_{3_i}^{t} \tag{26}$$

It is worth noting that both methods described here are solved explicitly. Consequently, these methods must be able to satisfy the stability condition. In this study, the authors employed the Courant number for testing the stability condition. Moreover, the suggested model has no limitation on the number of multi-species. However, the analytical solutions implemented here have used up to four species. Therefore, solutions for the four species are presented here.

Results and discussions

In the current research, to investigate the multi-species solute transport in porous media a numerical model is developed. The analytical results of three multi-species solute transport problems introduced by Pérez Guerrero et al., (2009) and Bauer et al., (2001) were employed to analyze the accuracy and efficiency of the presented numerical model with LWFDM and FOFDM. MATLAB was employed to build the suggested model.

The first two case studies used analytical outcomes of dimensionless concentration for a three-species nitrification chain ($NH_4^+ \rightarrow NO_2^- \rightarrow NO_3^-$). In the first case, the distance and duration of the problem were selected as 220cm and 200h, respectively. Also, in the second case, the distance and duration of the problem were applied as 110cm and 50h (much less time), respectively. The linear interpolation method is employed to calculate the essential interval values for analytical results. More details about these two case studies, for instance, decay coefficient (λ_m), retardation coefficient (R_m), initial and boundary conditions, are presented in Table (1). It is important to note that in all tables and figures below, the first two case studies are referred to as the analytical results of dimensionless concentration for the three-species nitrification chain ($NH_4^+ \rightarrow NO_2^- \rightarrow NO_3^-$) introduced by Pérez Guerrero et al., (2009) for 220cm, 200h and 110cm, 50h, respectively. Furthermore, case three is the analytical result of a four-member decay chain solute transport problem derived from the Bauer et al., (2001) study. Moreover, in all of the figures and tables below related to the two first cases, the x, c, curve_1, curve_2, and curve_3, are the abbreviations of distance (cm), concentration (mM), outcomes of analytical expressions introduced by Pérez Guerrero et al., (2009) for NH_4^+, outcomes of analytical expressions introduced by Pérez Guerrero et al., (2009) for NO_2^-, and outcomes of analytical expressions introduced by Pérez Guerrero et al., (2009) for NO_3^-, respectively. Also, LWFDM_C1, LWFDM _C2, LWFDM _C3, FOFDM_C1, FOFDM_C2, and FOFDM_C3 are the abbreviations of calculated dimensionless concentration with a suggested model for LWFDM for NH_4^+, calculated dimensionless concentration with a suggested model for LWFDM for NO_2^-, calculated dimensionless concentration with a suggested model for LWFDM for NO_3^-, calculated dimensionless concentration with suggested model for FOFDM for NH_4^+, calculated dimensionless concentration with suggested model for FOFDM for NO_2^-, and calculated dimensionless concentration with suggested model for FOFDM for NO_3^-, respectively.

Table 1. Parameter values for the nitrification chain problem

Description	NH_4^+ (m=1)	NO_2^- (m=2)	NO_3^- (m=3)
Retardation coefficient (R_m)	2	1	1
Decay coefficient, λ_m	0	0.1	0
First case→$C(x,1)$	0	0	0
First case→$C(1,t)$	0.9982064510	0.001731801827	0.00006174718691
First case→$C(N,t)$	1.199389159E-89	1.255589051E-12	0.0002545665546
Second case→$C(x,1)$	0	0	0
Second case→$C(1,t)$	0.9982064510	0.001731801827	0.00006174718691
Second case→$C(N,t)$	5.1438380E-177	1.622019705E-50	2.260630087E-48
Pore velocity=1 cmh⁻¹	Dispersion	coefficient	D=0.18cm²h⁻¹

The outcomes of numerical investigations for the first two case studies are illustrated in Figures (1) and (2) and Tables (2-4). The above-mentioned case studies are simulated with two space and time intervals. The first case is simulated in space (N_x) and time (N_t) with the (N_x=331, N_t= 800001) and (N_x=441, N_t=200001) number of nodes. Similarly, the second case is employed (N_x=221, N_t=250001), and (N_x=441, N_t=600001) numbers of nodes in space (N_x) and time (N_t) to solve the problem. The numerical results of the first case at a distance and time equal to 220cm and 200h for all the nitrogen species are illustrated in Figure (1). Besides, the numerical results of the second case at a distance and time equal to 110cm and 50h for all the nitrogen species are illustrated in Figure (2). Based on the numerical outcomes demonstrated in the figures, it can easily be seen that both LWFDM and FOFDM have calculated close results. Therefore, for benchmark purposes, the total mean square error (TMSE), L₂-, and L∞-norms are determined by the following relations. The outcomes of the comparisons are illustrated in Tables (2-4).

$$TMSE = \frac{\sum(c_{Numerical\ solution} - c_{analytical\ results})^2}{N} \tag{27}$$

$$||x||_2 = \sqrt{x_1^2 + x_2^2 + \cdots + x_{N-1}^2 + x_N^2} \tag{28}$$

$$||x||_\infty = max[|x_1|, |x_2|, \ldots, |x_N|] \tag{29}$$

The numerical solutions for decay chain transport in porous media are extensively applicable. "Although only radioactive decay is a true first-order process, also chemical and biological transformations can be often described approximately in terms of first-order decay" (Bauer et al., 2001). As mentioned earlier, based on the numerical results demonstrated in the tables below, it can be seen that both the LWFDM and FOFDM schemes can illustrate good agreements with the results of analytical values. To achieve a deeper focus on the applied schemes, the comparison of numerical results, one by one, is presented here. Regarding the first case study, the numerical results yielded in Table (2) show that the FOFDM in the first- (NH_4^+) and second-member (NO_2^-) determined slightly better results than LWFDM. Nevertheless, the numerical outcomes of L₂- and L∞-norms in Tables (3-4) demonstrate that LWFDM provides more accurate results. In the second case, generally, LWFDM obtains more precise results than FOFDM.
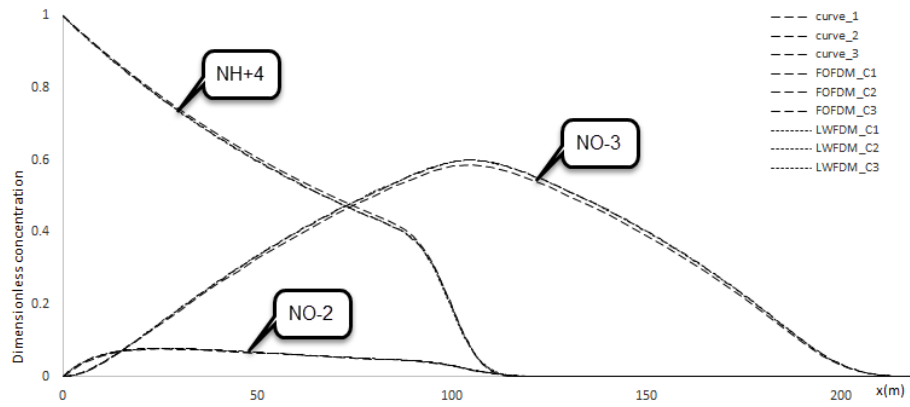
Fig. 1. Illustration of results of first case for 1D transient concentration distribution for all the nitrogen species (220cm and 200h) and (N_x=331, N_t=800001).
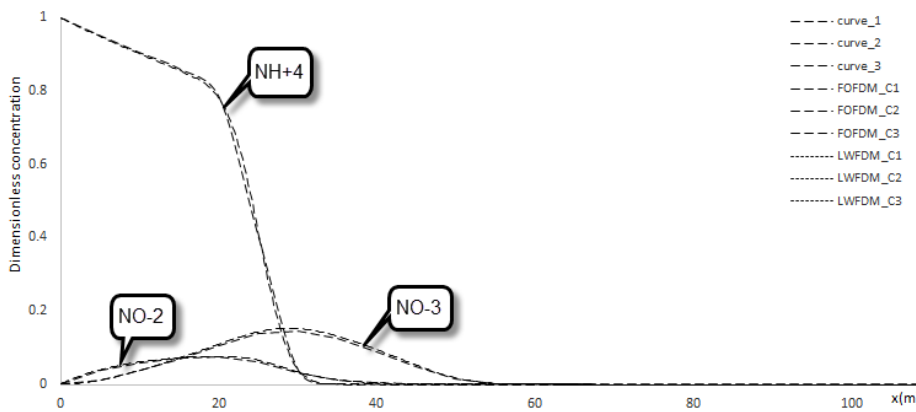

Fig. 2. Illustration of results of second case for 1D transient concentration distribution for all the nitrogen species (110cm and 50h) and (N_x=441, N_t=60001).

Table 2. Table of TMSE for the first and second cases

Description	Nx(Δx); Nt(Δt)	NH_4^+ (m=1)	NO_2^- (m=2)	NO_3^- (m=3)	Execution time(s)
First case→ LWFDM	331(0.6667);800001(0.00025)	2.92685E-05	1.11154E-06	8.06441E-05	2.92685E-05
First case→EFOFDM		2.55927E-05	1.03669E-06	8.21961E-05	512.807369
First case→ LWFDM	441(0.5);200001(0.001)	2.9121E-05	1.11681E-06	8.08962E-05	46.771354
First case→EFOFDM		2.65833E-05	1.06039E-06	8.19144E-05	145.763324
Second case→LWFDM	221(0.5);250001 (0.0002)	0.000138592	2.46814E-06	1.06738E-05	38.282872
Second case→EFOFDM		0.0001587	2.48433E-06	1.13168E-05	100.173238
Second case→LWFDM	441(0.25);600001(0.000083333)	0.000148592	2.52067E-06	1.08812E-05	226.570315
Second case→EFOFDM		0.000155325	2.51632E-06	1.11242E-05	437.070194

160

Table 3. Table of L$_2$-norms for the first and second cases

L$_2$-	Description	Nx(Δx); Nt(Δt)	NH_4^+ (m=1)	NO_2^- (m=2)	NO_3^- (m=3)
	Analytical results of equal interval node distribution	331(0.6667);800001(0.00025)	8.031114327	0.74391006	6.615388059
	LWFDM		7.95209243	0.760873	6.776044
	EFOFDM		7.960036905	0.76095	6.776169
First case	Analytical results of equal interval node distribution	441(0.5);200001(0.001)	9.264546037	0.85901057	7.638814144
	LWFDM		9.17326893	0.878634	7.824448
	EFOFDM		9.179941339	0.878695	7.824534
	Analytical results of equal interval node distribution	221(0.5);250001 (0.0002)	6.104308005	0.449497	0.912087457
	LWFDM		6.135397889	0.470967	0.958306
	EFOFDM		6.146293889	0.47112	0.958493
Second case	Analytical results of equal interval node distribution	441(0.25);600001(0.000083333)	8.603468	0.635614	1.289799
	LWFDM		8.649479357	0.666281	1.355536
	EFOFDM		8.656191449	0.66634	1.355607

Table 4. Table of L$_\infty$-norms for the first and second cases

L$_\infty$-	Description	Nx(Δx); Nt(Δt)	NH_4^+ (m=1)	NO_2^- (m=2)	NO_3^- (m=3)
	Analytical results of equal interval node distribution	331(0.6667);800001(0.00025)	0.991726725	0.077019	0.586836973
	LWFDM		0.991382	0.07902	0.598951
	EFOFDM		0.992145	0.079031	0.599018
First case	Analytical results of equal interval node distribution	441(0.5);200001(0.001)	0.993346656	0.077057	0.587139464
	LWFDM		0.993083	0.079027	0.598982
	EFOFDM		0.993638	0.079035	0.599027
	Analytical results of equal interval node distribution	221(0.5);250001 (0.0002)	0.993347	0.074712	0.146364487
	LWFDM		0.993083	0.077032	0.15312
	EFOFDM		0.993638	0.076832	0.153216
Second case	Analytical results of equal interval node distribution	441(0.25);600001(0.000083333)	0.995777	0.074712	0.146364
	LWFDM		0.995641	0.076886	0.153235
	EFOFDM		0.995895	0.07684	0.153253

In the final case study, an arbitrary decay chain containing four species in a complex porous medium at 3000 m and 3000 days is used. Application of these distance and time values reveals that the introduced model can suitably solve problems in the semi-infinite domain and long duration of time. The details of the problem for the third case study are illustrated in Table (5).

Moreover, in all of the figures and tables below related to the third case, the x is the abbreviation of distance (cm), c is the abbreviation of concentration (mM), C1, C2, C3, and C4, are the abbreviations of outcomes of analytical expressions for the concentration introduced by Bauer et al., (2001) for four species, LWFDM_C1, LWFDM _C2, LWFDM _C3, and LWFDM _C4, are the abbreviations of numerical results of the concentration with the suggested model for LWFDM for four species, and FOFDM_C1, FOFDM_C2, FOFDM_C3, and FOFDM_C4 are the abbreviations of numerical results of the concentration with the suggested model for FOFDM for four species, respectively. In case three, we carried out four numerical experiments to investigate the developed model more deeply, including N_x=1001, N_t=15001; N_x=1501, N_t=30001; N_x=2001, N_t=40001; and N_x=2001, N_t=60001. Parallel to the two first cases, the TMSE, L$_2$- and L$_\infty$-norms are calculated. The numerical results are

presented in Tables (6-8). The numerical outcomes of concentration distributions for the four-member decay chain for N_x=1001, and N_t=15001 in case three are demonstrated in Figure (3). The numerical results given in Table (6) show that in the third case, LWFDM calculates more reliable TMSE results than FOFDM. Numerical outcomes in Table (7) clarify that except the third-member, the results of LWFDM are more accurate, and numerical outcomes of Table (8) elucidate that except for third- and fourth-members, the results of LWFDM are more accurate. In conclusion, it can easily say that the numerical results of LWFDM for all cases are more accurate and reliable. Even in cases where FOFDM achieves better results, the differences are negligible. One of the main points behind the better performance of LWFDM in all case studies is related to the boundary conditions. As is evident to all, boundary conditions have a significant impact on the accuracy of numerical methods. FOFDM needs to consider more ghost node points than LWFDM. This fact affects, first of all, the accuracy of numerical results, and secondly, it makes the process of developing a model cumbersome. The last but not least point is that in all case studies, the required execution time for LWFDM is much shorter than the FOFDM.
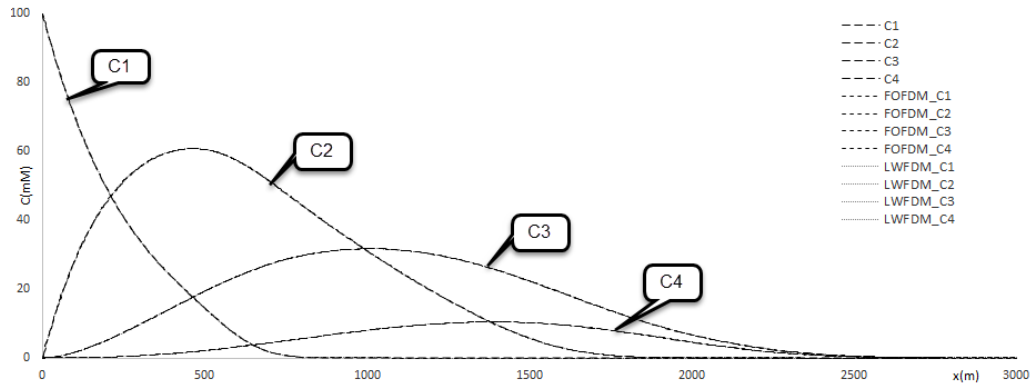

Fig. 3. 1D transient concentration distribution for constant boundary condition (3000m and 3000day) in (N_x=1001, N_t=15001).

Table 5. Parameter values for the third case

Description	C_1 (m=1)	C_2 (m=2)	C_3 (m=3)	C_4 (m=4)
Retardation coefficient (R_m)	5.3	1.9	1.2	1.3
Decay coefficient, $\lambda_m \times 10^{-4}$ (day^{-1})	7	5	4.5	3.8
Third case→$C(x,1)$ (mM)	0	0	0	0
Third case →$C(1,t)$ (mM)	100	0	0	0
Third case→$C(N,t)$ (mM)	0	0	0	0
Pore velocity=1 mday^{-1}	Dispersion	coefficient	D=10m^{2}day^{-1}	

Table 6. Table of TMSE for the third case

Description	Nx(Δx); Nt(Δt)	C₁ (m=1)	C₂ (m=2)	C₃ (m=3)	C₄ (m=4)	Execution time(s)
Third case→ LWFDM	1001(3);15001(0.2)	0.00341617	0.006046303	0.001608776	0.001715191	7.508856
Third case→EFOFDM		0.004821301	0.008065866	0.001719605	0.001823453	26.554933
Third case→ LWFDM	1501(2);30001(0.1)	0.003486966	0.006025762	0.001668566	0.00176801	21.480427
Third case→EFOFDM		0.00431609	0.00723868	0.001711212	0.001815357	88.527707
Third case→ LWFDM	2001(1.5);40001(0.075)	0.003565671	0.005966808	0.001686528	0.001782023	55.981296
Third case→EFOFDM		0.004144471	0.00682945	0.001717049	0.001818372	152.220120
Third case→ LWFDM	2001(1.5);60001(0.05)	0.003561612	0.005933962	0.001706274	0.001796552	57.247254
Third case→EFOFDM		0.004145105	0.006812481	0.001713147	0.001812118	202.831910

Table 7. Table of L₂-norms for the third case

L₂-	Description	Nx(Δx); Nt(Δt)	C₁ (m=1)	C₂ (m=2)	C₃ (m=3)	C₄ (m=4)
	Analytical results of equal interval node distribution	1001(3);15001(0.2)	677.3394	909.7015	566.1908	180.1968
	LWFDM		678.2099	909.6674	565.8571	179.7832
	EFOFDM		678.7518	909.7855	565.8606	179.7525
Third	Analytical results of equal interval node distribution	1501(2);30001(0.1)				
case			828.0354	1114.147	693.4388	220.6947
	LWFDM		829.0513	1114.154	693.005	220.1615
	EFOFDM		829.4979	1114.226	693.007	220.1427
	Analytical results of equal interval node distribution	2001(1.5);40001(0.075)	955.2477	1286.505	800.7144	254.8364
	LWFDM		956.4115	1286.528	799.0596	252.4782
	EFOFDM		956.7907	1286.589	799.0635	252.4662
	Analytical results of equal interval node distribution	2001(1.5);60001(0.05)	955.2477	1286.505	800.7144	254.8364
	LWFDM		956.3931	1286.538	799.0523	252.4712
	EFOFDM		956.7896	1286.58	799.0548	252.4627

Table 8. Table of L_∞-norms for the third case

L_∞-	Description	Nx(Δx); Nt(Δt)	C_1 (m=1)	C_2 (m=2)	C_3 (m=3)	C_4 (m=4)
Third case	Analytical results of equal interval node distribution	1001(3);15001(0.2)	98.22275	60.78184	31.70163	10.485
	LWFDM		98.93161	60.77521835	31.67349	10.4398
	EFOFDM		99.01777	60.79262064	31.67862	10.44122
	Analytical results of equal interval node distribution	1501(2);30001(0.1)	98.45076	60.78459	31.70348	10.485
	LWFDM		99.28634	60.78333125	31.67441	10.43943
	EFOFDM		99.34206	60.79199843	31.67697	10.44015
	Analytical results of equal interval node distribution	2001(1.5);40001(0.075)	98.56202	60.78432	31.70441	10.485
	LWFDM		99.46425	60.78531858	31.67464	10.43935
	EFOFDM		99.50531	60.79180174	31.67656	10.43989
	Analytical results of equal interval node distribution	2001(1.5);60001(0.05)	98.56202	60.78432	31.70441	10.485
	LWFDM		99.46423	60.78724772	31.67486	10.43927
	EFOFDM		99.50531	60.79155971	31.67614	10.43962

CONCLUSION

This paper documented the development of a new numerical model based on the two different schemes of FDM (i.e., LWFDM and FOFDM) that solved the multi-species solute transport phenomenon in porous media. Although there is no limitation on the number of multi-species, the analytical results of three different well-established problems (i.e., three-species ($NH_4^+ \rightarrow NO_2^- \rightarrow NO_3^-$) and four-species problems) were applied to evaluate the proposed model. TMSE, L_2- and L_∞ norms were used to analyze the numerical results accurately. Regarding the numerical results yielded in this paper, both the LWFDM and FOFDM have calculated acceptable results. The numerical experiments for all of the case studies were carried out with at least two various numbers of space- and time intervals. In the first case study, the numerical outcomes express that the FOFDM in the first-(NH_4^+) and second-member (NO_2^-) were determined slightly better results than LWFDM. On the other hand, the LWFDM was determined more accurate results for L_2- and L_∞-norms. In the last two cases, in general, LWFDM results are found to be more accurate than FOFDM. As a final point, it can be stated that in all case studies, the required execution time for LWFDM was much shorter than FOFDM. In conclusion, it can easily be said that the LWFDM is a more accurate and reliable method than the FOFDM.

ACKNOWLEDGEMENTS

REFERENCES

Bagalkot, N., & Kumar, G.S. 2015. Effect of nonlinear sorption on multispecies radionuclide transport in a coupled fracture-matrix system with variable fracture aperture: a numerical study, ISH Journal of Hydraulic Engineering, 21(3): 242–254.

Bauer, P., Attinger, S., & Kinzelbach, W. 2001. Transport of a decay chain in homogenous porous media: analytical solutions, Journal of Contaminant Hydrology, 49: 217–239.

Celiker, M. 2016. Determination of the interaction between groundwater and surface water using environmental isotopes (Oxygen-18, Deuterium and Tritium) and chemical analyses in Uluova Region, Elazig, Turkey, Journal of Engg. Research, 4(1):105-124.

Chen-Charpentier, B.M., Dimitrov, D.T., & Kojouharov, H.V. 2009. Numerical simulation of multi-species biofilms in porous media for different kinetics, Mathematics and Computers in Simulation, 79: 1846–1861.

Dalkiliç, H.Y., & Gharehbaghi A. 2021. Numerical modeling of groundwater flow based on explicit and fully implicit schemes of finite volume method, Journal of Engg. Research, 9 (4B):56-69, DOI:10.36909/jer.9253.

Das, P., Akhter, A., & Singh, M. K. 2018. Solute transport modelling with the variable temporally dependent boundary, Sadhana, 43(12):1-11.

Gharehbaghi, A. 2016. Explicit and implicit forms of differential quadrature method for advection–diffusion equation with variable coefficients in semi-infinite domain, journal of hydrology, 541: 935–940. http://dx.doi.org/10.1016/j.jhydrol.2016.08.002

Gharehbaghi, A. 2017. Third- and fifth-order finite volume schemes for advection–diffusion equation with variable coefficients in semi-infinite domain. Water and Environment Journal, 31(2): 184–193. doi:10.1111/wej.12233

Gharehbaghi, A., Kaya, B., & Tayfur, G. 2017. Comparative Analysis of Numerical Solutions of Advection-Diffusion Equation, Cumhuriyet University Science Journal (CSJ), 38(1):73-84. http://dx.doi.org/10.17776/csj.53808

Kaya, B., & Arisoy, Y. 2011. Differential Quadrature Solution for One-Dimensional Aquifer Flow, Mathematical and Computational Applications, 16(2): 524-534.

Kaya, B., & Gharehbaghi, A. 2014. Implicit Solutions of Advection Diffusion Equation by Various Numerical Methods. *Aust. J. Basic & Appl. Sci.,* 8(1), 381-391

Kumar, A., Kumar, D., & Kumar, J.N. 2010. Analytical solutions to one-dimensional advection–diffusion equation with variable coefficients in semi-infinite media. J. Hydrol. 380: 330–337.

Natarajan, N., & Kumar, S.G. 2010. Finite difference approach for modeling multispecies transport in porous media, International Journal of Engineering Science and Technology, 2(8): 3344-3350.

Pathania, T., Eldho, T.I., & Bottacin-Busolin, A. 2020. Coupled simulation of groundwater flow and multispecies reactive transport in an unconfined aquifer using the element-free Galerkin method, Engineering Analysis with Boundary Elements, 121: 31–49.

Pérez Guerrero, J.S., Skaggs, T.H., & van Genuchten, M.T. 2009. Analytical Solution for Multi-Species Contaminant Transport Subject to Sequential First-Order Decay Reactions in Finite Media, Transp. Porous Med, 80:373–387**.** DOI 10.1007/s11242-009-9368-3

Ramos, T.B., Simunek, J., Gonçalves, M.C., Martins, J.C., Prazeres, A., Castanheira, N.L., & Pereira, L.S. 2011. Field evaluation of a multicomponent solute transport model in soils irrigated with saline waters, Journal of Hydrology, 407(1–4): 129-144.

Savovic, S., & Djordjevich, A. 2012. Finite difference solution of the one-dimensional advection–diffusion equation with variable coefficients in semi-infinite media. Int. J. Heat Mass Transf. 55: 4291–4294. http://dx.doi.org/10.1016/j. ijheatmasstransfer.2012.03.073

Savovic, S., & Djordjevich, A. 2013. Numerical solution for temporally and spatially dependent solute dispersion of pulse type input concentration in semi-infinite media. Int. J. Heat Mass Transf. 60, 291–295. http://dx.doi.org/10.1016/j.ijheatmasstransfer.2013.01.027

Savovic, S., Djordjevich, A., Tse, P.W., & Nikezic, D., 2011. Explicit finite difference solution of the diffusion equation describing the flow of radon through soil, Applied Radiation and Isotopes, 69: 237–240. doi:10.1016/j.apradiso.2010.09.007

Sharma, A., Guleria, A., & Swami, D. 2016. Numerical modelling of multispecies solute transport in porous media, Hydro 2016 international conference, 159-169.

Singh, M.K., Ahamad, S., & Singh, V. P. 2012. Analytical Solution for One-Dimensional Solute Dispersion with Time-Dependent Source Concentration along Uniform Groundwater Flow in a Homogeneous Porous Formation, Journal of Engineering Mechanics,138(8).1045-1056

Torlapati, J. 2013. Development and Application of One Dimensional Multi-Component Reactive Transport Models, Phd. dissertation, Alabama

Zhang, Z.h., Zhang, J.P., Ju, Z.Y., & Zhu, M. 2018. A one-dimensional transport model for multi-component solute in saturated soil, Water Science and Engineering, 11(3): 236-242.